Physics – Uspekhi **66** (12) 1248 – 1257 (2023)

INSTRUMENTS AND METHODS OF INVESTIGATION PACS numbers: 61..05.C –, 68.37.Hk, 68.37.Lp, 78.70.Gq

Potential of the microwave method for the activation of carbon materials in comparison with the traditional thermal method

I G Dyachkova, D A Zolotov, A S Kumskov, I S Volchkov, V V Berestov, E V Matveev

DOI: https://doi.org/10.3367/UFNe.2023.02.039323

Contents

Abstract. Microwave exposure is one possible promising heating method that can be used to create porous carbon materials. Activated carbon materials obtained by microwave heating can serve as an adsorbent or electrode material in energy storage devices such as supercapacitors. The paper investigates the processes of carbonization and activation of cotton lint using microwaves. A comparison is made with the traditional thermal method of heating, as well as with the mass-produced highly porous carbon fiber Busofit T1.

Keywords: cotton lint, Busofit, microwaves, carbonization, activation, electron microscopy, X-ray phase analysis, adsorption activity

1. Introduction

Over the past two decades, much research has been conducted to find efficient ways to convert waste and biomass into valuable products. The development of carbon-containing materials, activated carbon materials (ACMs), in particular, is among the most promising solutions. ACMs represent a new generation of materials with unique thermal, mechanical, and electrical properties, as well as new functional capacities. They have a customizable surface texture and functionality, possess the ability to form a large specific surface area (more than 3000 $m^2\ g^{-1}$) [1], and show high adsorption activity [2], good porosity [3], and high mechanical strength [4]. ACMs make up an important class of porous materials finding numerous applications in industrial processes, such as water and air purification [5–7] and gas storage and separation [8, 9]. These materials are also widely used as adsorbents [10, 11], in supercapacitors [12, 13], in composites [14], in chemical sensors [15], in medicine and catalysis [17, 18], etc.

The large specific surface area of ACMs, their optimal pore size, and their high electrical conductivity are fundamental properties for the construction of highly efficient supercapacitors [19]. The textural and structural properties of ACMs are attributable to the nature of their precursors, the methods and conditions of carbonization and activation, as well as subsequent processing. Today, optimization of characteristics of these materials is sought almost empirically. However, it is possible, based on experimental data, to select materials with properties intended for specific applications.

The variety of ACM precursors is great. Formally, all raw materials can be divided into two groups: those obtained from fossil sources and bio-raw materials [20–23]. The use of agricultural waste to make active charcoal reduces the cost of its production. Traditionally, the production of porous carbon materials is based on the thermochemical processes of pyrolysis and activation at temperatures of 300–1000 °C; they are accompanied by a number of complex reactions and transformations, leading to the formation of a carbon mass with highly developed porosity and, accordingly, a large surface area. Thus, provided the availability and diversity of bio-raw materials and waste rich in organic matter for the synthesis of ACMs, the economic efficiency of their industrial production is determined by the processes of heating and sometimes washing (chemical activation) [24]. Bearing in mind the growing demand for ACMs and the development of new technologies using these materials [25], reducing energy costs and environmental impacts of the processes involved in their production and regeneration is of paramount importance in the context of the current energy and

I G Dyachkova [(1, a)], **D A Zolotov** [(1, b)], **A S Kumskov** [(1, c)], **I S Volchkov** [(1, d)], **V V Berestov** [(2, e)], **E V Matveev** [(2, f)]
[(1)] Federal Scientific Research Center Crystallography and Photonics, Russian Academy of Sciences, Leninskii prosp. 59, 119333 Moscow, Russian Federation
[(2)] Research Institute of Advanced Materials and Technologies, ul. Shcherbakovskaya 53, 105187 Moscow, Russian Federation
E-mail: [(a)] sig74@mail.ru, [(b)] zolotovden@crys.ras.ru, [(c)] a.kumskov@gmail.com, [(d)] Volch2862@gmail.com, [(e)] vberestov97@gmail.com, [(f)] maegor@gmail.com

Received 26 December 2022, revised 14 February 2023
Uspekhi Fizicheskikh Nauk **193** (12) 1325 – 1334 (2023)
Translated by Yu V Morozov

environmental situation. Since the microwave effect on dielectric objects has a number of advantages (targeted, volumetric, and inertia-free heating) over traditional methods of high-temperature treatment, microwave heating appears to be an energy-efficient alternative for obtaining ACMs.

The main goal of the present paper was to study the synthesis of inexpensive and high-quality activated carbon materials from cotton fluff, a waste product from textile production. For this purpose, different carbonization and activation modalities were used, including traditional thermal heating and the new microwave technique with special emphasis on its influence on the structure and properties of the final product in comparison with the traditional method. We used a comparative analysis of the samples obtained by the microwave method and of those produced by the traditional (thermal) one (including samples of the commercially produced Busofit T-1 carbon fiber sorbent). In this case, the two-stage carbonization/activation process performed using the thermal method implies by default 'full' activation, characterized by the high uniformity of properties (such as adsorption, morphology, porosity, elemental composition) throughout the entire volume of the sample. These characteristics are taken as the initial ones in the comparison with the results of microwave carbonization. At the same time, microwave carbonization gives rise, due to the high rates of the processes, to the formation of a structure with properties less uniform throughout the sample volume if compared to that obtained by the thermal method. In particular, the volume of such a sample contains areas (conventionally called 'black'), the properties of which (adsorption activity, black color intensity, elemental composition, microstructure, etc.) correspond to those of samples that have undergone carbonization and activation by the traditional method. The presence of areas with similar properties during microwave carbonization allows the conclusion that activation occurs partly together with carbonization (in the thermal processing method, these processes are separated).

To determine and compare the physicochemical properties of activated carbon materials obtained by different methods, the following methods were used: electron microscopy, X-ray phase analysis (XPA), and measurement of adsorption activity.

2. Description of samples

We studied samples obtained during carbonization (with subsequent activation) of cotton fluff (waste from textile production) by thermal and microwave methods, as well as a serial sample of Busofit T-1 (an activated carbon fabric; see Table 1).

The starting material was cotton fluff balls having a dry weight of 3.0 g each.

Carbonization and partial activation by the microwave technique were carried out in a collapsible quartz reactor installed inside a specialized microwave chamber [26]. Carbonization and subsequent activation by the thermal method were performed inside an LF-50/500-1200 tubular electric furnace using standard technology [26]. For more intensive carbonization of the raw material, orthophosphoric acid H_3PO_4 was used as a chemical activating agent. It is known that dehydrating agents, such as orthophosphoric acid, interacting with components of plant biomass catalyze dehydration and condensation reactions known to maintain carbonization of the material and thereby increase the yield of the carbonized product and decrease the elemental oxygen content [27].

Argon gas was used to provide an inert atmosphere. After carbonization and activation, the resulting samples were weighed on laboratory scales of class II accuracy. The microwave carbonization and activation modes were selected empirically based on preliminary studies, and the completion of the activation stage was determined from the residual mass of the sample and the presence of black areas. We made use of the black areas concept only in relation to microwave-carbonized samples. Areas of two shades (intense black and graphite-gray) could be visually distinguished in the volume of such samples. Presumably, the greater intensity of the 'black color' in partially activated areas is due to the more developed surface of carbonized fibers that absorbs light more readily than the areas that failed to undergo activation (they look grayer owing to their less developed surface and the presence of deposited impurity elements).

At the same time, samples that have undergone two-stage carbonization and thermal activation have, by default, a uniformly deep black color, as confirmed both visually and instrumentally.

Table 1. Study samples and their residual mass, regimes, and conditions of treatment.

No.	Name	Impregnation	Treatment	m, g	Notes
1	Original	Dry fluff	—	3.0	Cotton fluff balls
2	Original, treated with a 5% H_3PO_4 solution	5% H_3PO_4 Wet fluff	—	—	Impregnated wet fluff
3	MW-K	5% H_3PO_4 Wet fluff	$10'Ar + 10'CO_2$	0.785	Impregnated wet fluff. No black areas
4	MW-A	3% H_3PO_4 Dried fluff	$5'CO_2 + 120''$ air	0.308	Impregnated dried fluff. Total carbonization in the chamber; many black areas
5	T-K	5% H_3PO_4 Wet fluff	Heating from 20 to 900 °C at a rate of 10°C min^{-1} in an Ar flow of 0.8 l min^{-1} ($\sim$ 50 min)	0.945	Only carbonization
6	T-A	5% H_3PO_4 Wet fluff	In a CO_2 flow of 0.8 l min^{-1} at 900 °C (40 min)	0.286	Carbonization with subsequent activation
7	B-A	—	Commercial product	—	Busofit T-1 (CF-based sorbent)

Carbonization of a cotton fluff sample impregnated with 5% H_3PO_4 (Microwave-C) was carried out at an Ar flow rate of 0.8 l min^{-1} for 10 min and in a CO_2 atmosphere during the same time at a microwave power of $\sim$ 500 W. The weight of the sample after carbonization amounted to 0.785 g. To perform microwave carbonization with partial activation, a sample of cotton fluff (microwave-A) was soaked in a 3% H_3PO_4 solution in a water bath for 60 min, after which it was dried for 24 hours. The carbonization process with partial activation was carried out in two stages: in the CO_2 atmosphere for 5 min, then in the air for 120 s at a microwave power of $\sim$ 500 W. The mass of the sample after activation was 0.308 g.

Thermal carbonization of a cotton sample (T-K) soaked in 5% H_3PO_4 was carried out in an Ar flow of 0.8 l min^{-1} for 50 min while heated from 20 to 900 °C at a rate of 10°C min^{-1}. The mass of the sample after carbonization was 0.945 g. Subsequent thermal activation of the carbonized sample (T-A) was carried out in CO_2 at 900 °C and a flow rate of 0.8 l min^{-1} for 40 min. The mass of the sample after activation was 0.286 g.

Because the most common and popular carbon-based materials are fabrics, Busofit-type carbon fabric (CF) was used in this work. Comparative studies were carried out using the activated carbon fabric Busofit T-1 (B-A), produced by Khimvolokno JSC (Svetlogorsk, Republic of Belarus). It is a highly porous carbon fiber consisting of thin threads (5–15 μm in diameter) formed largely by carbon atoms. This fabric has high tensile strength and a low specific gravity and thermal expansion coefficient; it is chemically inert and has a large specific surface area (1130 m^2 g^{-1} as determined by the BET procedure) with a pore volume of 0.3–0.8 cm^3 g^{-1} [28]. The adsorption activity, estimated using methylene blue, is not less than 300 mg g^{-1}.

3. Research methods

3.1 Electron microscopy

The fiber structure in carbon materials was studied by scanning electron microscopy (SEM), scanning transmission electron microscopy (STEM), transmission electron microscopy (TEM), and energy-dispersive X-ray microanalysis (EDXMA). We used an FEI Scios autoemissive scanning electron-ion microscope (Thermo Fisher Scientific, USA), the secondary electron mode at accelerating voltages from 2 to 20 kV, and a FEI Tecnai Osiris field transmission electron microscope (Thermo Fisher Scientific, USA) at an accelerating voltage of 200 kV. A transmission electron microscope was equipped with a special system of detectors, allowing maps of the distribution of chemical elements to be obtained. For TEM studies, samples were placed on copper grids with a thin amorphous carbon substrate.

3.2 X-ray phase analysis

To determine the phase composition and calculate the crystalline to amorphous phase ratio, samples of carbon materials were examined using a MiniFlex 600 X-ray diffractometer (Rigaku, Japan). The source of radiation was an X-ray tube with a copper anode (CuK$_\alpha$, $\lambda = 1.54$ Å) at an accelerating voltage of 40 kV and a current of 15 mA. The measurements were made in the Bragg–Brentano geometry in the $\theta - 2\theta$ scanning mode. The angle interval 2θ was 5–60° with a step of 0.01° and exposition of 1 s per step. The ICDD PDF-4 database [29] was used to identify phases.

3.3 Adsorption activity

The adsorption activity of carbon material samples following carbonization and activation was determined by the spectrophotometric method with the use of methylene blue (MB) as the indicator [30]. Methylthioninium chloride, usually called methylene blue, is a salt used as a dye. The amount of dye adsorbed from the solution during contact with the sorbent (carbon material) was measured using a calibration curve. The concentration of substances in the aqueous solution was determined by measuring optical density in a cuvette with a 1-mm-thick adsorbing layer during maximum MB adsorption at a wavelength of 665 nm. Time-dependent MB adsorption was studied under static conditions with periodic stirring at the sorbent/solution ratio of 1:10.

The adsorption activity (X, mg g^{-1}) was calculated using MB as the indicator and the formula

$$X = \frac{(C_1 - C_2 K)\, 0.025}{m}\,, \qquad (1)$$

where C_1 is the mass concentration of the initial indicator solution [mg l^{-1}], C_2 is the mass concentration of the solution after its clarification by the sample material [mg l^{-1}], K is the dilution factor ($K = 10$), 0.025 is the volume of the indicator solution taken for clarification [l], and m is the mass of the sample [g].

The procedure for the analysis and calculation of adsorption activity of the samples using an indicator is described in detail in [31].

4. Results and discussion

SEM shows that samples of the original cotton fluff, as well as those treated with a 5% H_3PO_4 solution, are 7-to-20-μm-wide fibers twisting towards the center (Figs 1a, 2a). The fibrillar structure is well apparent on the fiber surface of both samples. The fibrils are located parallel to one another and twist in a helical manner at an angle relative to the fiber axis.

TEM studies of individual fibrils in a sample of the original cotton fluff revealed that they have an elongated shape and a diameter of $\sim$ 150–350 nm. In general, they are homogeneous and amorphous, and have mesopores measuring 10–20 nm (Fig. 1b). The fibrils of cotton fluff samples treated with the 5% H_3PO_4 solution have a similar shape and mesopores (Fig. 2b). STEM images of the fibrils show that they are decorated with nanoparticles (Figs 1c, 2c).

Element distribution maps (Figs 1d, 2d) and energy-dispersive X-ray spectra (Figs 3a, b) indicate the predominance of carbon and/or its oxide in original samples and confirm the presence of chlorine, calcium, magnesium, and oxygen; they also reveal carbon and/or its oxide, phosphorus, calcium, silicon, and oxygen in the samples treated with the 5% H_3PO_4 solution.

The presence of copper peaks in all examined EDXA spectra is attributable to the use of a copper grid in electron microscopic studies.

According to the results of an X-ray fluorescence (XRF) analysis, a sample of the original cotton fluff consists of three phases: the most intense carbon phase, which is amorphous (C-amorphous) judging by the shape of the peaks, and more crystalline calcium (Ca) and graphite (C-graphite) phases (Fig. 4a). It can be assumed, taking into consideration the

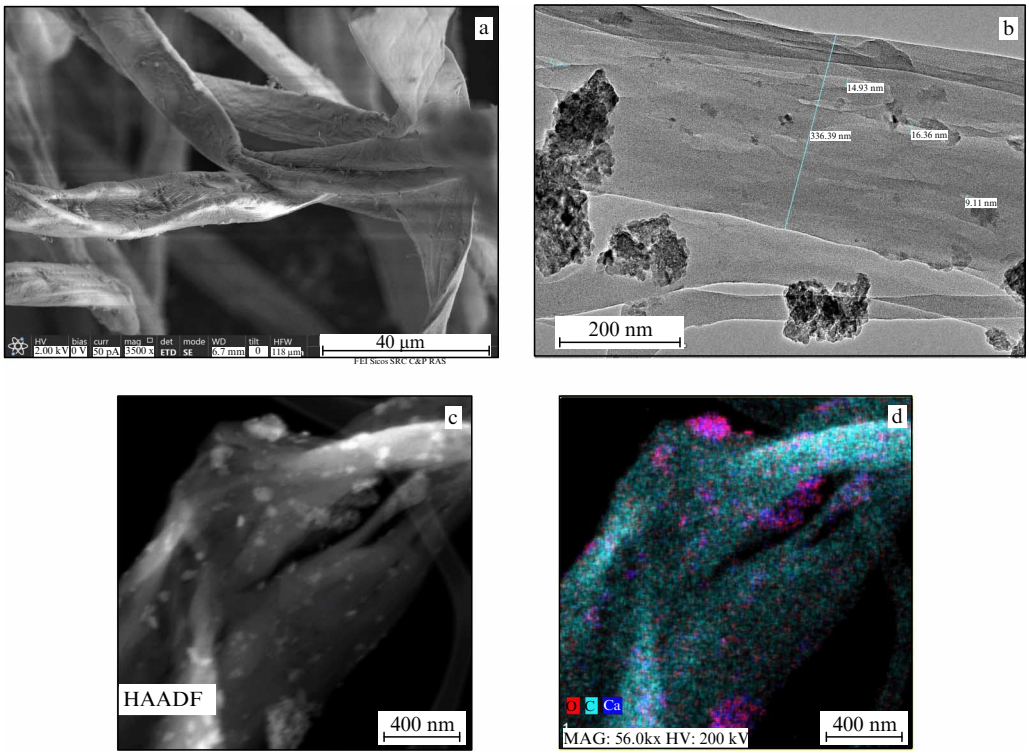

Figure 1. Original cotton fluff: (a) SEM image, general view; (b) TEM image of single fibrils; (c) STEM image, location of elemental analysis; (d) element distribution map.

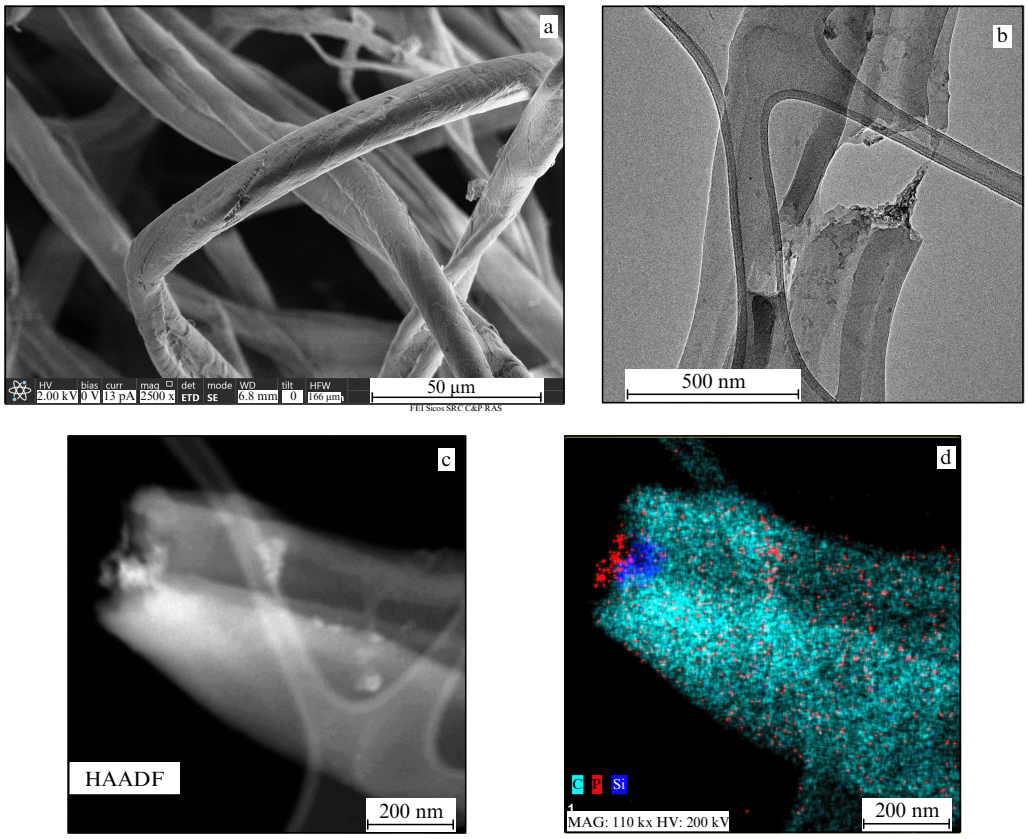

Figure 2. Cotton fluff treated with a 5% H_3PO_4 solution: (a) SEM image, general view; (b) TEM image of single fibrils; (c) STEM image, location of elemental analysis; (d) element distribution map.

nature of the sample, that amorphous carbon forms a layer of the 'shell' of the cotton threads that make up the sample. Graphite and calcium are located under this layer. As a result, reflections from them are less intense. This is partially

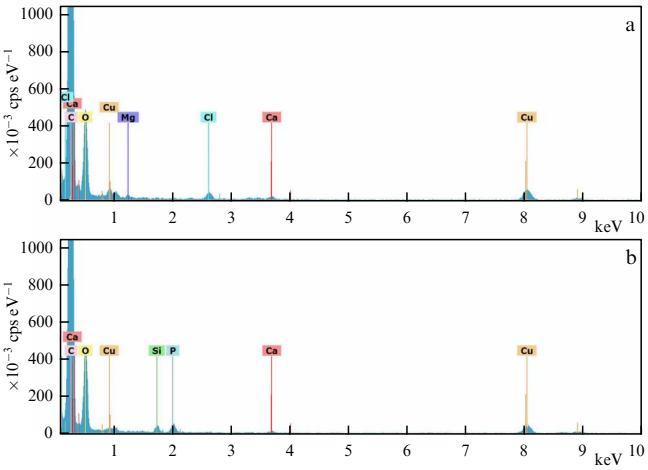

Figure 3. EDXMA spectra: (a) original sample; (b) 5% H_3PO_4-treated sample.

confirmed by the results of TEM and SEM studies as more local in nature. An element distribution map obtained using EDXA (Fig. 1d) demonstrates a continuous distribution of carbon over the sample, while only isolated areas of local calcium accumulation can be seen. It is worth noting that the intensity of reflexes is related not only to the location of the phases but also to their number. Obviously, the sample under consideration is rich in the amorphous carbon phase.

XRF shows that a sample of cotton fluff treated with 5% H_3PO_4 consists of the same phases found in the original sample (Fig. 4b). Notably, the intensity of the peaks corresponding to individual phases differs. That of the peaks of amorphous carbon is significantly decreased, whereas the intensity of the C and Ca peaks is increased. Moreover, three new peaks presumably corresponding to $Ca(H_2PO_4)_2$ (calcium hydrogen phosphate) appear (Fig. 4b). It can be assumed that the treatment of the original cotton fluff with a 5% H_3PO_4 solution leads to the partial dissolution of the shell consisting of amorphous carbon. Thereafter, the H_3PO_4 solution reacts with local Ca accumulations, the number of which markedly increases after the thinning of the amorphous carbon layer, which gives rise to new phases (a reaction like $2H_3PO_4 + Ca \rightarrow H_2 + Ca(H_2PO_4)_2$). The partially etched structure of the sample treated with the 5% H_3PO_4 solution is quite apparent in the TEM image (Fig. 2b), which indirectly confirms the assumption of the dissolution of a part of the amorphous carbon shell in the 5% H_3PO_4 solution.

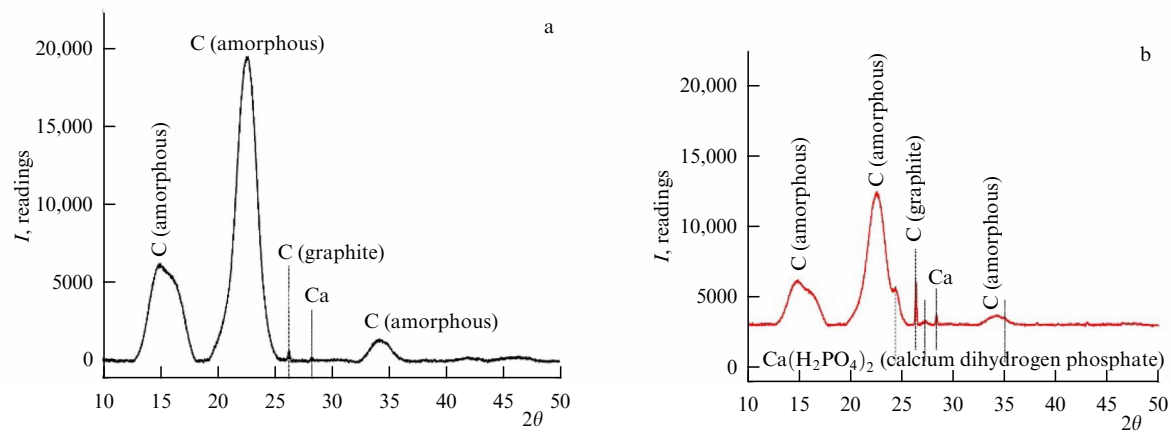

Figure 4. X-ray diffraction patterns of cotton fluff samples: (a) initial; (b) soaked in a 5% solution of orthophosphoric acid H_3PO_4.

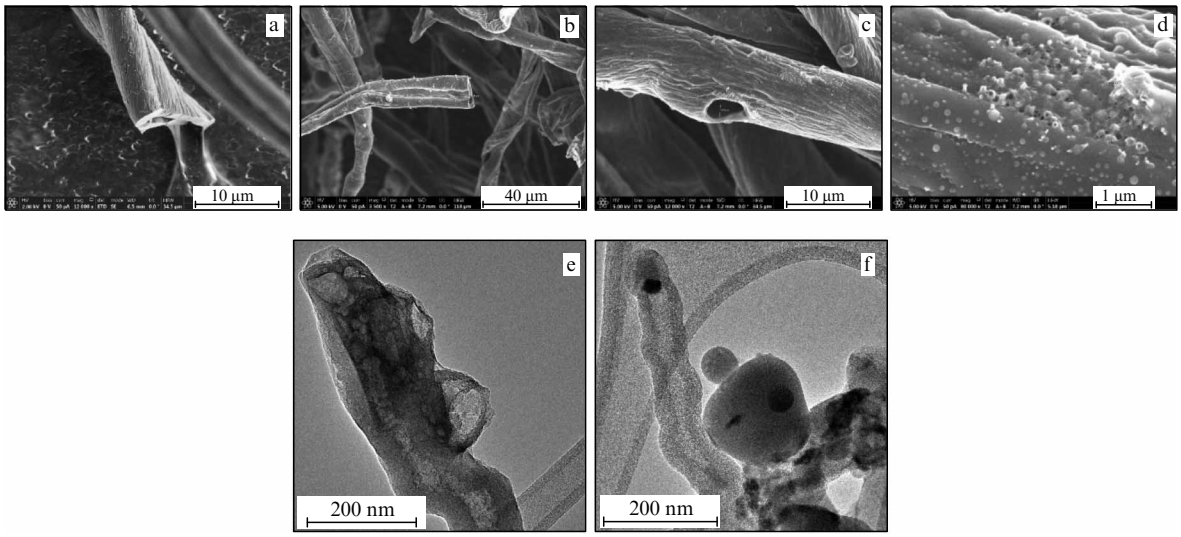

Figure 5. Carbonized cotton fluff fibers: (a) SEM image of the T-K sample; (b–d) SEM image of the microwave-K sample; (e) TEM image of the microwave-K sample; (f) TEM image of the T-K sample.

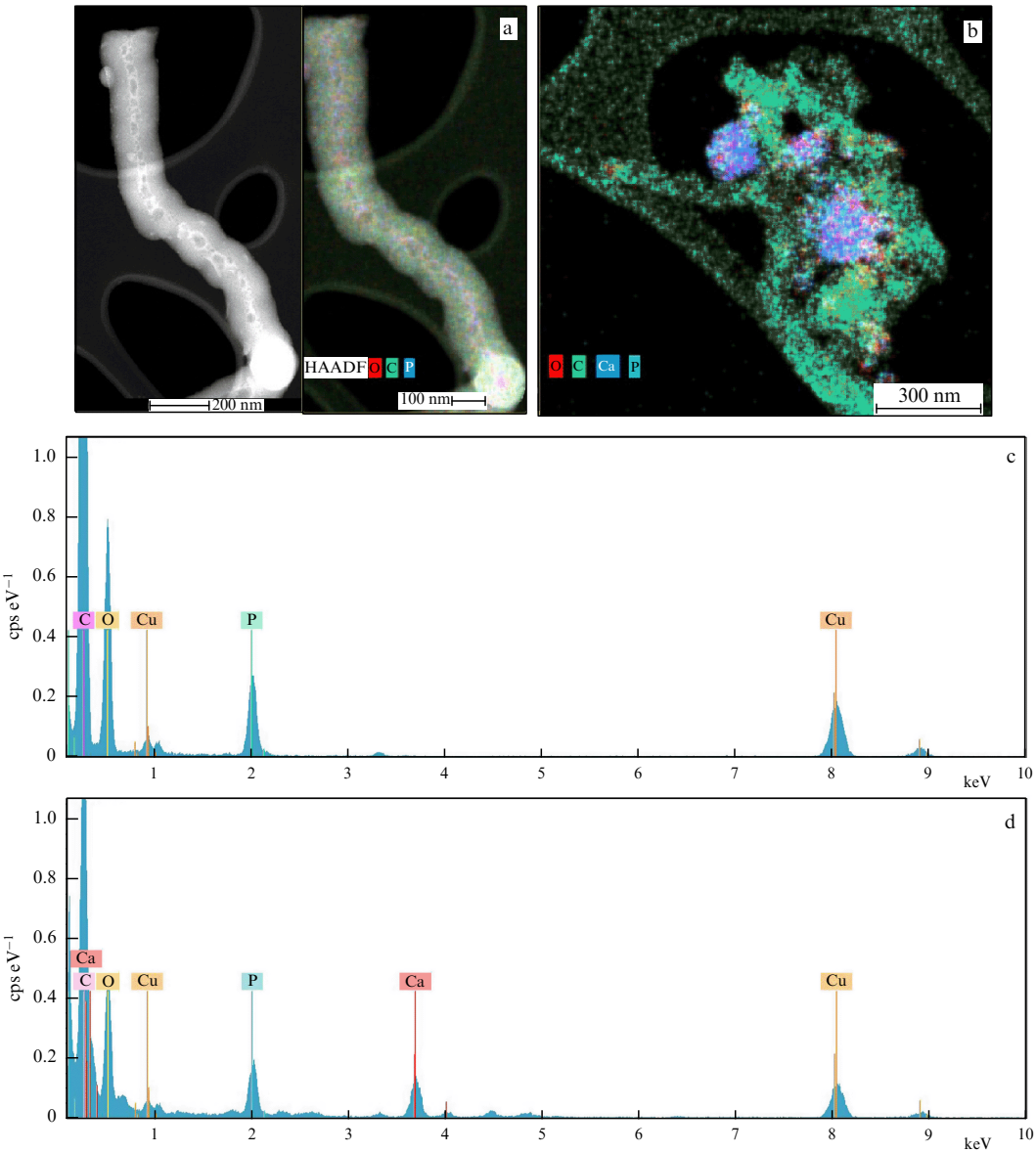

Figure 6. EDXMA analysis of carbonized cotton fluff: (a) STEM image and element distribution map of the microwave-K sample; (b) element distribution map of the T-K sample; (c) EDXMA spectrum of the microwave-K sample; (d) EDXMA spectrum of the T-K sample.

SEM revealed the following structural features of carbonized cotton fluff samples. The fiber width in T-K samples ranges from 5 to 20 μm, and the fiber wall thickness amounts to 300–800 nm (Fig. 5a), while in microwave-K samples it undergoes thinning to ∼ 300–500 nm (Fig. 5b). These data fairly well correlate with the measured masses of the carbonized samples, since the residual mass of a T-K sample is 17% higher than that of a microwave-K sample. Moreover, micropores with a size of 2–7 μm (Fig. 5c) and mesopores sized 10–110 nm (Fig. 5d) are found in the fiber walls of the microwave-K sample.

TEM studies of individual fibrils of carbonized samples showed that they are mostly homogeneous, amorphous, elongated, and 50–200 nm in diameter (Fig. 5e, f). Some of them have an internal channel with a diameter of 20–50 nm. In the fibrils of a microwave-K sample, mesopores measuring 5–60 nm are present (Fig. 5e). In a T-K sample, fibrils decorated with nanoparticles 100–200 nm in diameter can be seen (Fig. 5f).

The element distribution maps (Fig. 6a, b) and EDXA spectra (Fig. 6c, d) suggest the predominance of carbon, phosphorus, and/or their oxides in carbonized samples; also, they confirm the presence of oxygen. Nanoparticles found in T-K samples consist of calcium, phosphorus, and/or their oxides (Fig. 6b).

XRF gives evidence that the MW-K sample (microwave-carbonized) is totally amorphous (Fig. 7a). Its structure is very similar to the X-ray diffraction pattern of glass carbon or carbon dioxide, which can also be amorphous, as shown by SEM and TEM studies. The respective images (Fig. 5b, c, e) demonstrate that the general structure of the sample is of the shell/core type, while the general structure of the shell resembles that of an annealed thin film. X-ray phase analysis (XPA) (Fig. 7a), like EDXA (Fig. 6c), failed to confirm the presence of calcium and did not show the presence of crystalline graphite. Judging by the position of the peaks in the diffraction pattern, amorphous carbon makes up the main phase in microwave-K samples.

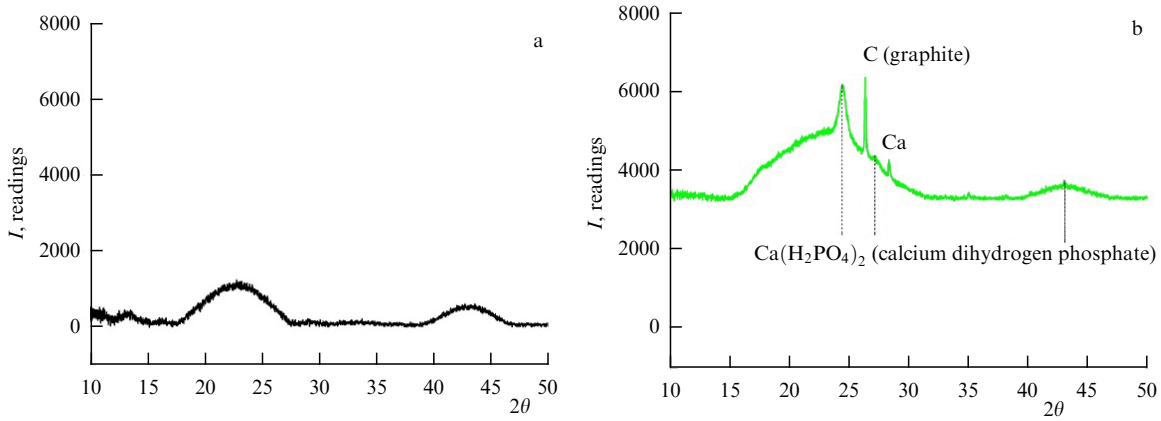

Figure 7. Diffraction patterns of carbonized cotton fluff samples: (a) MW-K; (b) T-K.

XPA of the diffraction pattern of a thermally carbonized T-K sample (Fig. 7b) showed its similarity to that of a microwave-K sample in terms of the presence of amorphous halos characteristic of glassy carbon or carbon dioxide. In particular, the peaks of graphite, calcium, and calcium dihydrogen phosphate are clearly visible in the X-ray diffraction pattern, which may be due to the processing conditions. Both the T-K sample and the microwave-K sample were processed in a mixed $CO_2 + Ar$ environment. However, the T-K sample was processed not only in the mixed atmosphere but also under heating. This accounts for the presence in this sample of both an amorphous mass characteristic of the MW-K sample and a crystalline mass consisting of a mixture of calcium, graphite, and calcium dihydrogen phosphate, as is readily noticeable in the SEM image (Fig. 5a), showing its 'fusion' with the amorphous mass of the main massive. It can be speculated that the carbon mass undergoes oxidation in a mixed medium in the absence of thermal heating, which gives rise to a thick carbon shell. Heating either prevents complete 'oxidation' or causes the amorphous film to disintegrate.

SEM studies of activated samples revealed the following structural features. The MW-A sample (microwave-activated) consists of fibers twisting towards the center and having an internal channel with a diameter of 0.8–2.2 μm and a width of 2–7 μm, i.e., almost three times smaller than the width of the fibers in MW-K samples. There is an unambiguous correlation with the difference in the residual mass. That of the microwave-K sample is 2.5 times greater than the residual mass of the MW-A sample. A fibrillar structure is quite apparent on the fiber surface. The fibers have pores 0.5–1.2 μm in size (Fig. 8a).

The structure of T-A samples (thermally activated) is formed by two types of fibers. One is represented by the fibers twisting toward the center and having a well-apparent fibrillar structure on the surface with or without an internal channel. The width of the fibers is 5–10 μm, which is half the width of those in the T-K sample. The second type is much smaller; the fibers have neither a fibrillar structure nor internal channels. Their multiple pores are 0.11–1.33 μm in size (Fig. 8e).

Finally, the B-A sample (Busofit activated) consists of fibers with a diameter of 3–8 μm and a large number a pores measuring 50–200 nm. The fibrillar structure is clearly visible on the surface of the fibers. The fibrils are located parallel to each other (Fig. 8h).

TEM shows that individual fibrils of the microwave-A sample have a diameter of 50–120 nm (Fig. 8b), i.e., four times smaller than in the T-A sample (200–480 nm) (Fig. 8f). The diameter of fibrils in the B-A sample is 50–300 nm (Fig. 8i). Some fibrils have an internal channel as well as mesopores that are 20–50 nm in size in the microwave-A sample (Fig. 8b) and 30–200 nm in the T-A one (Fig. 8f). The fibrils of the B-A sample are saturated with mesopores 10–70 nm in size (Fig. 8i). In microwave-A (Fig. 8c) and B-A (Fig. 8j) samples, multi-walled carbon nanotubes (MWCNTs) are found. In T-A and T-K samples, individual fibrils are decorated with calcium nanoparticles 100–200 nm in diameter or such particles fill the fibril channels (Fig. 8g).

An analysis of results of electron microscopic studies reveals the main structural features of all activated samples, such as an increased concentration of mesopores and the presence of multi-walled carbon nanotubes in microwave-A and B-A samples.

MW-A and B-A samples are similar in terms of elemental composition (Fig. 8d) and (Fig. 8k). Both contain carbon and oxygen, but the former include in addition phosphorus as a consequence of their impregnation with orthophosphoric acid. In the T-A sample, carbon, phosphorus, calcium, silicon, and oxygen predominate (Fig. 8g). The intercalating element is calcium. The observed particles consist of calcium, phosphorus, and/or their oxides.

Figure 9 shows diffraction patterns of all three activated samples of carbon materials under study. XPA demonstrated a faint amorphous halo in the MW-A sample (Fig. 9a) corresponding to that in the MW-K and T-K samples, as well as an insignificant peak at 17.44° (2θ) similar to one of the $Ca_3(HP_2O_7)_2$ peaks observed in the T-A and B-A samples. The microwave-A sample shows calcium, graphite-2H, and calcium hydrogen phosphate peaks. There is no carbolite phase. It can be assumed that the conditions for the formation of a structure similar to that of the B-A sample correspond to those used in processing microwave-A and T-A samples. However, in the case of the microwave-A sample, the exposure was insufficient, as is indirectly evidenced by the presence of an amorphous halo, suggesting that the amorphous phase did not have enough time to 'decompose.'

The diffraction patterns of the microwave-A sample presented in Fig. 9b exhibit three peaks characteristic of MWCNTs [(002), (100), and (004)], with the strongest one

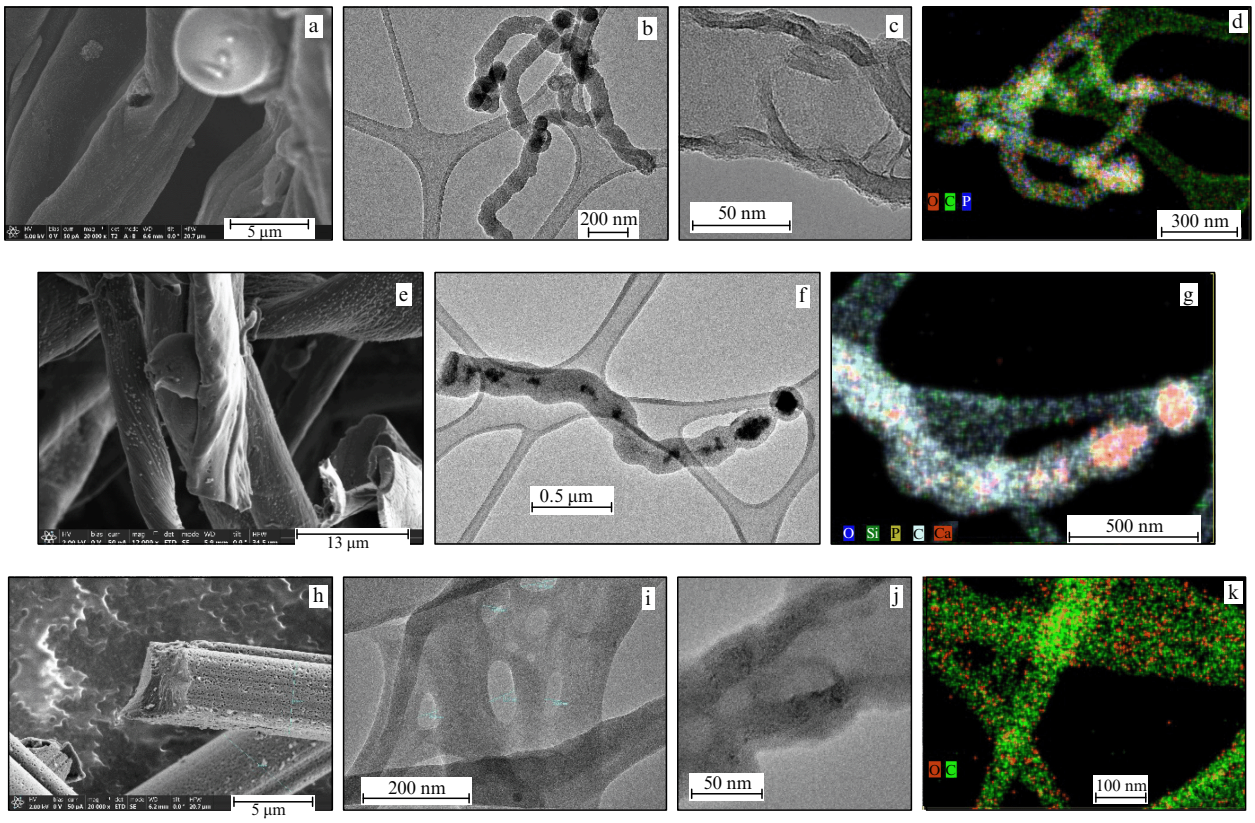

Figure 8. Activated samples: (a) SEM image of the microwave-A sample; (b) TEM image of the microwave-A sample; (c) TEM image of MWCNT in a microwave-A sample; (d) element distribution map of the microwave-A sample; (e) SEM image of the T-A sample; (f) TEM image of the T-A sample; (g) element distribution map of the T-A sample; (h) SEM image of the B-A sample; (i) TEM image of the B-A sample; (j) TEM image of MWCNTs with conical walls in the B-A sample; (k) element distribution map of the B-A sample.

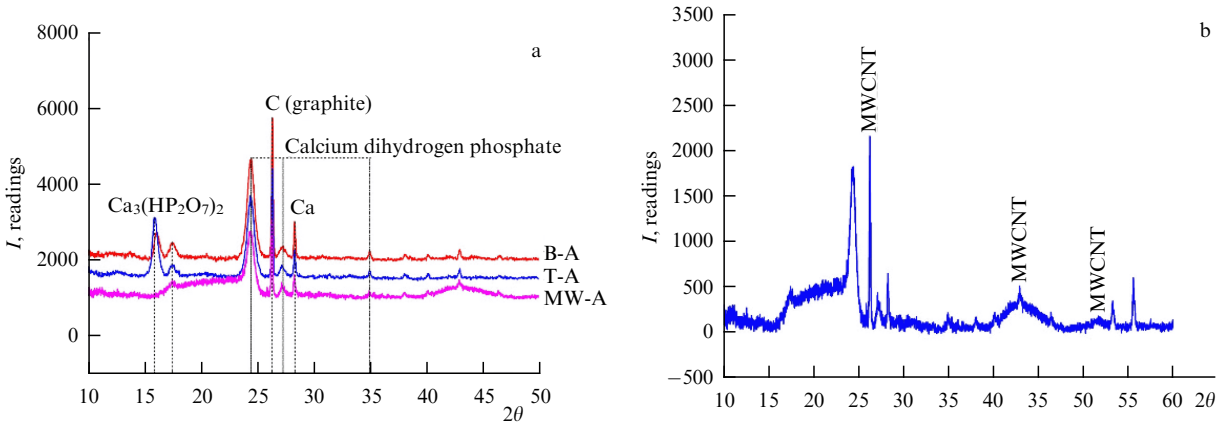

Figure 9. X-ray diffraction patterns of activated samples: (a) microwave-A, T-A, B-A (spaced along the ordinate); (b) MWCNT peaks for the microwave-A sample.

located at an angle of 26.3° in the graphite spectrum corresponding to the diffraction on the planes formed by its sp^2-carbon layers (graphene layers). It should be noted that the asymmetric peak in the region of $2\theta = 11.7°$, characteristic of amorphous carbon structures, is absent; low-intensity peaks at angles of 44° and 54° can be attributed to MWCNTs (100) and (004), respectively. According to the results of the X-ray phase analysis, the structure of the microwave-A sample shows a higher degree of amorphism of the graphite-like phase than the structure of T-A and B-A samples, which may suggest the presence of MWCNTs in microwave-A samples, since multi-walled carbon nanotubes are more amorphous than crystalline carbon or graphite.

XPA demonstrated excellent agreement between X-ray diffraction patterns of B-A and T-A samples. Both produce peaks corresponding to graphite, calcium, and calcium dihydrogen phosphate phases. Also, additional peaks appear that probably correspond to the $Ca_3(HP_2O_7)_2$ phase. This phase is synthetic and forms, under ideal conditions, upon $Ca(H_2PO_4)_2$ annealing in the air at 240 °C for an hour. The temperature of this procedure is higher than under the reference conditions for the formation of the $Ca_3(HP_2O_7)_2$

phase; however, the environment in which the annealing occurs differs from the reference one.

It is noteworthy that SEM analysis revealed pores in the fibers of T-A and B-A samples (Figs 8e and 8h, respectively) that are likely to be areas of $Ca(H_2PO_4)_2$ accumulation, giving rise to a new phase under the influence of the ongoing reaction. Such areas are most frequently present in T-A and B-A samples and less frequently in MW-A ones (Fig. 8a). In the fibers of B-A samples, such areas look more like 'burns' resulting from an exothermic reaction. In T-A samples, they are larger but fewer than in their B-A counterparts, and they do not occupy the entire surface of the fiber. Probably, the upper layer of the fibers in these samples consists of $Ca(H_2PO_4)_2$, which begins to be 'etched' in the course of local formation of the new phase.

Finally, the adsorption activity of all samples carbonized and activated by different methods was determined by MS (Table 2).

Table 2. Adsorption activity of the study samples.

Sample	Adsorption activity X, mg g^{-1}
MW-K (MW-carbonized)	< 100
T-K (thermally carbonized)	20
MW-A (MW-activated)	452
T-A (thermally activated)	577
Commercial B-A sample (busofit)	300

The adsorption activity of the samples was determined immediately after carbonization and activation of the material. The data obtained indicate that the adsorption activity of MW-carbonized samples was almost five times that of thermally carbonized ones. Also, thermal carbonization took 2.5 times more time than microwave carbonization (50 vs 20 min).

After the MW treatment in the CO_2 atmosphere for 5 min and in two stages (1 min each) in the air, areas of intense black color characteristic of activated carbons appeared in the parts of the samples exposed to elevated temperature. The adsorption activity of such areas determined by MS amounted to 451.6 mg g^{-1}, i.e., it was comparable to the activity of thermally activated samples (576.84 mg g^{-1}) and the commercial carbon fiber sorbent Busofit T-1 (300.44 mg g^{-1}). This allowed concluding that there is a relationship (positive correlation) between the intensity of the 'black' color and the adsorption activity, which suggests partial activation in these areas. The greater intensity of the 'black' color in partially activated areas may be due to the more developed surface of cotton fibers with the growing number of nano-, meso-, and micropores. Such a surface more actively absorbs visible light than do graphite-gray areas that do not have such a developed surface.

Note that the appearance of areas with a deep black color and increased adsorption activity (partial activation) during microwave treatment occur in one stage (in the CO_2 atmosphere and in the air), in contrast to thermal activation, which needs two stages (carbonization + activation) to occur with the substitution of CO_2 for Ar. In this case, the time spent on microwave treatment to obtain a partially activated sample was 7 min, while it took 90 min for thermal activation, with a greater yield of the finished material: 0.308 g for microwave activation and 0.286 g for thermal activation.

5. Conclusion

We undertook comparative studies of the surface morphology, elemental, and adsorption activity of cotton fluff fibers subjected to microwave and heat treatment for the purpose of carbonization and subsequent activation of the material. In addition, the commercial carbon fiber sorbent Busofit T-1 was investigated.

It was concluded based on the results of SEM and TEM studies that all activated samples have a highly porous amorphous structure of the fiber surface. MW-A samples (20–50 nm) have the optimal size of mesopores close to that in serial Busofit T-1 samples (10–70 nm) which characterizes good adsorbents. Moreover, thermally activated samples contain more impurities, which entails an additional stage of their purification.

The formation of multi-walled carbon nanotubes in microwave-activated samples was documented by analogy with serial Busofit, meaning that microwave heating is a promising method for creating nanotubes in ACM. Their nano-size tubular morphology provides a developed specific surface area of an activated carbon material. The specific surface area of carbon nanotubes is mainly due to the presence of mesopores and is associated with the outer surface of the tubes and the cavities arising from intertwined nanotubes and, sometimes, owing to the presence of a central channel, so that most of the pores in the material form a network of intertwined nanotubes. In other words, an activated carbon material containing nanotubes is characterized by well-developed meso- and microporosity responsible for its enhanced adsorption activity [32].

Results of the experimental analysis of activated samples allow a conclusion that cotton fluff (textile waste) can be used as a potential economical raw material for the production of activated carbon materials. The testing of various modes of the microwave method demonstrated that carbonization of the entire volume of a cotton fluff sample weighing 3 g impregnated with orthophosphoric acid takes 20 min if performed in two successive stages in Ar and CO_2 environments. The microwave method using H_3PO_4 as the activating agent is well suited for producing activated carbon materials from the cotton fluff. It has also been shown that microwave activation can be carried out in a single stage in the CO_2 atmosphere, in contrast to the classical thermal method, to speed up and, accordingly, reduce the cost of the ACM production process.

Acknowledgments. The study was carried out in the framework of the State Assignment to the Federal Research Center Crystallography and Photonics, Russian Academy of Sciences, in the part concerning electronic and X-ray research in the framework of the assignment to the Ministry of Science and Higher Education of the Russian Federation FNER-2022-0002 in the part related to obtaining carbon samples and studying adsorption activity.

References

1. Daud W M A W, Ali W S W, Sulaiman M Z *Carbon* **38** 1925 (2000)
2. Chen Y et al. *Adv. Colloid Interface Sci.* **163** 39 (2011)
3. Malik R, Ramteke D S, Wate S R *Waste Management* **27** 1129 (2007)
4. Acharya J et al. *Chem. Eng. J.* **150** 25 (2009)
5. Namasivayam C, Kavitha D *Dyes Pigments* **54** 47 (2002)
6. Abdelkader A et al. *Appl. Petrochem. Res.* **11** 137 (2021)

7. Prakash M O et al. *Mater. Today Proc.* **39** 1476 (2021)
8. Marsh H, Rodríguez-Reinoso F *Activated Carbon* (Amsterdam: Elsevier, 2006)
9. Bansal R C, Goyal M *Activated Carbon Adsorption* (Boca Raton, FL: Taylor and Francis, 2005)
10. Lu C, Su F *Separat. Purificat. Technol.* **58** 113 (2007)
11. Pal A et al. *Appl. Thermal Eng.* **122** 389 (2017)
12. Cuentas-Gallegos A K et al. *Electrochem. Commun.* **9** 2088 (2007)
13. Teo E Y L et al. *Electrochim. Acta* **192** 110 (2016)
14. Shim B S, Starkovich J, Kotov N *Composit. Sci. Technol.* **66** 1174 (2006)
15. Vaezi M R, Sadrnezhaad S K *Mater. Sci. Eng. B* **140** 73 (2007)
16. Bottani E J, Tascón J M D (Eds) *Adsorption by Carbons* (Amsterdam: Elsevier, 2011)
17. Raymundo-Piñero E, Leroux F, Béguin F *Adv. Mater.* **18** 1877 (2006)
18. Wang L, Schnepp Z, Titirici M M *J. Mater. Chem. A* **1** 5269 (2013)
19. Li Z, Xu K, Pan Y *Nanotechnol. Rev.* **8** (1) 35 (2019)
20. Kwiatkowski J F (Ed.) *Activated Carbon*: *Classifications, Properties and Applications* (New York: Nova Sci. Publ., 2011)
21. Ioannidou O, Zabaniotou A *Renew. Sustain. Energy Rev.* **11** 1966 (2007)
22. González-García P *Renew. Sustain. Energy Rev.* **82** 1393 (2018)
23. Danish M, Ahmad T *Renew. Sustain. Energy Rev.* **87** 1 (2018)
24. Kumar N S et al. *Renew. Sustain. Energy Rev.* **124** 109743 (2020)
25. Wang X et al. *Chemosphere* **287** 131995 (2022)
26. Matveev E V et al. *Inorg. Mater. Appl. Res.* **13** 549 (2022); *Perspektivnye Mater.* (11) 54 (2021)
27. Vervikishko D E "Korrelyatsii mezhdu nanoporistoi strukturoi uglerodnykh materialov i funktsional'nymi kharakteristikami superkondensatorov na ikh osnove" ("Correlations between the nanoporous structure of carbon materials and functional characteristics of supercapacitors based on them"), Thesis for Cand. Tech. Sci. (Moscow: Joint Institute for High Temperatures, RAS, 2014)
28. Zolotukhin I V, Kalinin Yu E *Uglerodnye Nanotrubki i Nanovolokna* (Carbon Nanotubes and Nanofibers) (Voronezh: Voronezh. Gos. Tekh. Univ., 2006)
29. Gates-Rector S, Blanton T *Powder Diffraction* **34** 352 (2019)
30. GOST 4453-74. Ugol' aktivnyi osvetlyayushchii drevesnyi poroshkoobraznyi. Tekhnicheskie usloviya. (GOST 4453-74. Active charcoal brightening wood powder. Technical conditions). Date of introduction 1976-01-01, https://www.gostinfo.ru/catalog/Details/?id=4163182
31. Asadchikov V E et al. *Crystallogr. Rep.* **67** 556 (2022); *Kristallografiya* **67** 597 (2022)
32. Shornikova O N, Maksimova N V, Avdeev V V *Svyazuyushchie dlya Polimernykh Kompozitsionnykh Materialov* (Binders for Polymer Composite Materials) (Moscow: MGU, 2010)